Microcrack Testing and Monitoring Using FBGS for Hydrogen Tanks

MIGUEL GONZALEZ DEL VAL,
JOSE MANUEL MARTINEZ OLMO,
JAVIER GONZALEZ GONZALEZ,
OLGA ANGELA SALAZAR CASTAMAN,
FERNANDO CABRERIZO and MALTE FROVEL

ABSTRACT

The transition toward zero-emission aviation demands the development of lightweight and safe storage systems for cryogenic hydrogen. Type V composite tanks, which lack a metallic or polymeric liner, offer significant advantages in terms of mass reduction and thermal compatibility. However, their long-term viability is challenged by hydrogen permeability due to matrix microcracking, which can occur under cryogenic conditions and compromise tank integrity. This study explores an indirect method to assess microcrack formation by measuring the thermal expansion behavior of a composite laminate. Using controlled thermal cycles and induced damage scenarios, changes in the coefficient of thermal expansion (CTE) were monitored and correlated with internal microcracking. Results demonstrate a measurable and repeatable variation in thermal expansion after damage, supporting its use as a structural health monitoring (SHM) indicator. The findings provide a promising path toward the implementation of non-destructive techniques for in-service integrity assessment of Type V hydrogen tanks.

INTRODUCTION

Hydrogen has gained importance in the last years as a solution for the next generation Zero zero-emission aircraft [1]. However, a few improvements must be made before the technology can be fully implemented. Aspects like hydrogen embrittlement, efficiency performance, or safety are critical for the technology development [2]. There are multiple developments in new hydrogen tanks that are more lightweight and implementable in the aeronautical sector, considering aspects like cost or safety. New hydrogen tank ideas, specifically in Type III and Type IV tanks have been implemented during the last years, including solutions for fuel cells or Liquid Hydrogen. Moreover, there is an increasing interest in the manufacturing of new Type V tanks without any liner, so there are not any thermal expansion or additional stresses between the liner and the composite material that can provoke failure [3]. There are additional hydrogen embrittlement problems related to metals [4] that make more attractive type V tanks instead of metal liner solutions.

The liner's main function is, not only being used as a support in filament winding manufacturing and for structural porpuses but also serves as a shield for hydrogen permeation [5]. One of the main problems of hydrogen Type V tanks is the leakage and permeability that can have critical consequences on safety [6]. Leakage drastically affects aspects like durability [7] or safety and is a key point in hydrogen storage [8]. Even when the Type V pressure vessels are the most interesting in terms of weight and efficiency, leakage is the principal disadvantage so those type of tanks are still in the design phase.

Leakage, in the case of composite materials, is mainly provoked by matrix microcracking in the 90º plies [9]. Cracks serve as pathways to hydrogen, so they drastically deteriorate the laminate's performance. In reference [10], a dependence between permeability and strain state was established, seeing a probable influence of microcracking. Thermoplastics, due to their higher ductility and recyclability, are trying to be implemented without a large success [11].

Miguel Gonzalez: gonzalezvm@inta.es INTA Carretera de Ajalvir km 4 Torrejon de Ardoz, Madrid Spain

Knowing that leakage due to microcracking is the most likely cause of failure, detecting microcracking is one important aspect of monitoring a hydrogen tank. Furthermore, mandatory very high safety factors (2.5 with de ultimate strength according to [12]) due to the hydrogen inherent risk and the use of very conservative strength estimations, make SHM a useful tool for reducing structural weight and safety factors [2].

Several works have reported SHM technologies for damage detection in filament winding structures [13] reported an Integrated Health Monitoring Concept applicable to cryogenic reusable tanks analytically. In this particular work, a diagnosis model was implemented with a study of the different SHM technologies and their possible application in cryogenic tanks. In reference, [14] SHM based on a piezoelectric system was placed in a panel with thermal adhesive characterization. In the case of reference [15], the same approach was done with a filament winding deposit, and integrating a smart layer of piezoelectric sensors inside the tank walls.

Among all SHM methods applicable to tanks, Fiber Optics are very attractive due to their electromagnetic nonsusceptibility and their low weight and size [16]. FBGS were previously used for strain measurement in cryogenic tests [17]. There have been acoustic emission experiments using fiber optics [18] that could be able to detect the crack emission, but this kind of system requires a large amount of data. The problem with FBGS is that it monitors strain and could be useful for a Load Monitoring System [19] and a prognosis system, but it cannot be implemented for a microcracking system. Moreover, it would be necessary to establish a relationship between microcracking and strain measured by the sensors.

The first possibility of monitoring microcracking is to measure the strains in a laminate and establish maximum strain criteria depending on the ply thickness. The main problem with this approach is that the transverse stress in a 90º laminate differs depending on variables like ply thickness or orientation of adjacent laminaes [20, 21]. Instead, energy methods are more commonly used for predicting microcracking, and the maximum strain criteria cannot be implemented [22, 23].

According to [21], there can be a variation between the thermomechanical properties and the existence of microcracking, so changes in the laminate mechanical properties can be related to internal cracking of the laminate. The main issue would be establishing a relationship between microcracking (and therefore leakage) and the thermomechanical properties. Microcracking affects several thermomechanical properties like thermal expansion [24, 25] or elastic constants [26, 27], so this fact could be used as a detection parameter.

MATERIALS AND METHODS

Problem statement

Unlike other applications, where mechanical properties such as stiffness or strength are paramount, hydrogen tanks' primary concern is their leakage resistance. So in this case failure would not be determined by its ability to carry a load but by the ability not to leak hydrogen and therefore ensure a safe operation. This is significantly influenced by the extent of internal microcracking of the inner tank, which can create specific hydrogen pathways that result in intolerable leaks and would completely vanish the high vacuum isolation between inner and outer tank.

Two different effective properties were thought to be measured. On the one hand, the different stiffness modulus, and on the other hand, the laminate thermal expansion. The first option was to detect the microcracking using stiffness because the detection could be done using internal pressure as a reference. It is easy to monitor the relationship between the strains and the pressure in a healthy and damaged structure. That option was not realistic because using normal damage models [28] for carbon cross-plies shows that the stiffness reduction is not significant. On the other hand, references like [25] show that there are very big differences in thermal expansion coefficients in a cross-ply laminate subjected to loading.

The problem observed in [25] is that there is an influence of the applied loads on the laminate and the observed coefficient of thermal expansion (CTE). Therefore, the testing in this paper will be conducted using only thermal loads, as this variation in the CTE could be exaggerated if loads were applied to the laminate. These thermal loads are caused by the large temperature variations of the laminate, typical of operations with hydrogen at cryogenic temperatures. The results obtained by [25] were also experimentally validated in reference [24]. The CTE can be measured during the operation of an inner liquid H2 aircraft tank by measuring the local strains, the temperature, and the inner pressure. The temperature changes typically from 20K in the full tank to about 70K in the almost empty tank. The technique described in

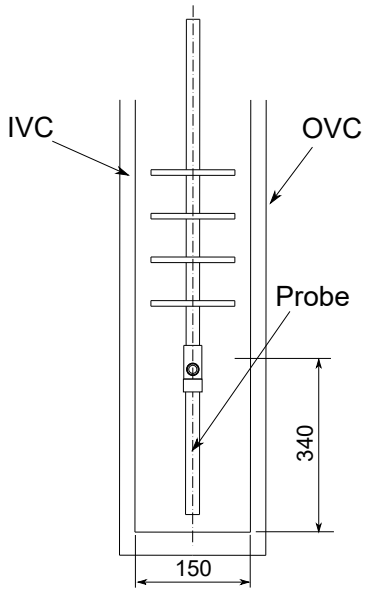

Figure 1. Cryostat Assembly diagram. IVT: Inner Vacuum Case. OVT: Outer Vacuum Case.

this paper could allow us to assess the microcracking condition of the inner tank in service and introduce maintenance operations before the microcracking state of the tank laminate becomes a serious problem.

Test Description

The probe used for the tests will be an IMA/M21 CFRP material [29] specimen with dimensions 230x30x1.3 mm. The specimen was similar to an ASTM D3039-type specimen with E-glass fiber-reinforced polymer matrix tabs. The probe width was larger than in other cases to adapt it to the permeability tests with a mass spectrometer.

The experimental procedure will be as follows. First, the thermal expansion curve of the laminate will be obtained from 20 K to room temperature. This way, the initial thermal stresses related to the heating of the laminate can be determined. Subsequently, the laminate will be cooled to 20 K and subjected to 35 cycles at 3000 microstrains to crack the internal structure. Finally, the thermal expansion will be measured in a manner quite similar to the previous one. Microcracking is induced at 20 K because, knowing that the resin loses toughness at low temperatures, it can be deduced that it will have a greater tendency to crack at these temperatures.

The tests were executed using INTA OXFORD cryostat, model 100KN, S/N 40786, with a scheme as seen in figure 1. To accurately determine the temperature within the equipment, a silicone diode sensor DT-600 [30] was strategically placed inside the cryostat and in contact with the probe using aluminum tape. The temperature measurements were recorded using Lakeshore 218 equipment connected to the computer.

For the thermal expansion calculation, FBGS was used using a similar procedure to [31]. Two fibers were bonded to the probe with two gratings each, in the directions ± 45 and $(0, 90)$. The fibers were Ormocer-coated, provided by FBGS TECHNOLOGIES, and bonded with an EA2A adhesive from Tokyo Measuring Instruments. The optical interrogator used for the testing was LUNA Si155. The spectrum at different temperatures is reported in Figure 2.

The extensometer used in the loading was an Epsilon LG10 [32]that can resist cryogenic temperatures and was recently calibrated by Instron. During the loading cycles, the displacement slope was 1 mm/min, and the testing temperatures were between 18 and 24 K.

Three loading cycle repetitions were conducted, with strain employed as the control parameter in each case. Table I details the maximum strain set for each repetition. In the first repetition, the strain was measured by the FBG oriented in 0º, and in the second and third repetitions, the strain was measured by

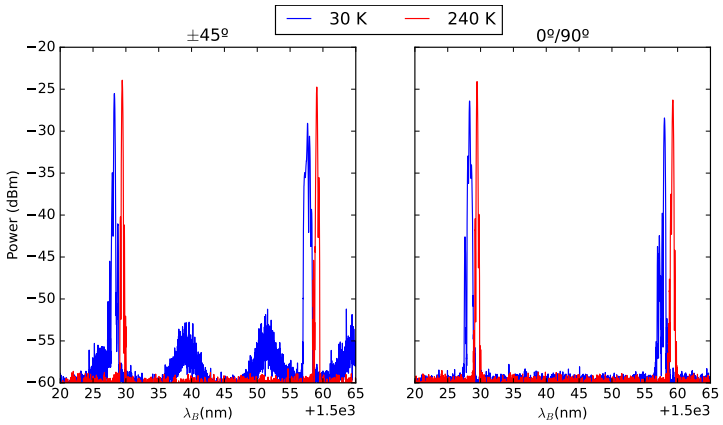

Figure 2. Spectrum of the two fibers used during the tests. In the case of the 0º/90º fiber, the first grating corresponds to the 90º direction, and the other grating to the 0º direction.

an LG10 extensometer.

Mathematical Formulation

Taking the starting point from the reference [33] and assuming that, from a micromechanical point of view, the effective coefficient of thermal expansion can be defined as:

$$\alpha_{ij}^{*} = \frac{1}{\sigma_{ij}^{0} V} \int_{V} \alpha_{ij}(\mathbf{x}) \sigma_{ij}^{s}(\mathbf{x}) \tag{1}$$

Where m represents each phase present in the material. It can therefore be observed that the effective thermal expansion can be decomposed according to the phase. Thus, the internal stresses of the laminate must be determined. In [34], it is assumed that the internal stresses of the laminate are the sum of the inherent stresses of a healthy laminate and the perturbed stresses of a cracked laminate. Therefore, the following expressions can be stated [25]:

$$\sigma_{ij}^{S} = \sigma_{ij}^{l} + \sigma_{ij}^{\prime} \tag{2}$$

By substituting equation 2 into equation 1, it can be determined that:

$$\alpha_{ij}^{*} = \alpha_{ij}^{0} + \frac{1}{V} \int_{V} \alpha_{ij} \sigma_{ij}^{\prime} dV \tag{3}$$

In the present work, the perturbation of the stresses is computed using a variational approach initially proposed by [34] for cross-ply laminates and later extended by [35] to angle-ply laminates. This method involves minimizing the complementary energy while enforcing the boundary conditions, which include traction continuity at the interfaces, symmetry in the (x, y) plane, and stress-free conditions on the external surfaces. To ensure these boundary conditions are satisfied, appropriate shape functions are employed in the calculation of the stress perturbations.

Being a symmetric laminate, the plies most affected by cracking are those located at the center of the laminate, as they have twice the thickness. The stress state is derived from the thermal strains of the specimen. For this purpose, the cracking stresses are calculated using equation 3, where the stresses indicated in the equation correspond to the perturbation thermal strain [25].

$$\begin{aligned} \int_{V} \alpha_{ij} \sigma_{ij}^{\prime} dV = & \int_{-a}^{a} \int_{-b}^{b} \int_{0}^{h_1} \left(\alpha_x \sigma_{xx}^{(1)} + \alpha_y \sigma_{yy}^{(1)} + \alpha_z \sigma_{zz}^{(1)} \right) dx\, dy\, dz + \\ & + \int_{-a}^{a} \int_{-b}^{b} \int_{h_1}^{h_1+h_2} \left(\alpha_x \sigma_{xx}^{(2)} + \alpha_y \sigma_{yy}^{(2)} + \alpha_z \sigma_{zz}^{(2)} \right) dx\, dy\, dz \end{aligned} \tag{4}$$

TABLE I. Number of cycles and maximum strain of each cycle in all repetitions

Repetition	Cycles	Maximum strain (μm/m)
1	30	800
2	34	3000
3	30	5000

The parameters a and b represent the distances between cracks, defining a bounded control volume. The stresses $\sigma_{xx}^{(n)}$, $\sigma_{yy}^{(n)}$, and $\sigma_{zz}^{n)}$ are expressed as internal stresses resulting from thermal strain in the n ply, being (1) the ply in the midplane and (2) the adjacent plies. The internal stress is represented using shape functions as described in [35]. The constants of the shape functions are determined from the strain measurements obtained with Fiber Bragg Gratings during the heating process from 20 K to room temperature. The analytical calculation of the effective coefficient of thermal expansion is out of the scope of the present article. Still, it is essential to highlight that an analytical relationship between the variation of the CTE and the distance between cracks can be established.

RESULTS

Although the thermal expansion coefficient is typically used to express the thermal dilation of materials in composite materials, due to the wider temperature range in these tests, another variable has been employed—namely, the thermal strain within a reasonable interval—to better represent the thermal expansion being investigated. The expansion responses have been compared in the three directions 0 and ± 45, and significantly different behaviors have been calculated depending on the number of applied thermal cycles. As mentioned before, the specimen was tested by cooling it down to 20 K and then allowing it to warm up very slowly, so thermal inertia issues are not expected.

The heating results can be visualized in Figure 3, which shows the material response in three different states (before the first cycle, after the first cycle, and after the second cycle). One of the main issues is that the optical spectra were broadened in low temperatures, likely due to a strain gradient in the grating bonded to the specimen. To address this, each grating was assigned a wavelength range, and within that range, the most prominent peak was detected using the *find_peaks* function from Python's *scipy* package.

A noticeably different behavior is observed depending on the specimen's state. A clear decrease in the thermal expansion coefficient is seen as more cycles with higher loads are applied. This trend is consistent with the results reported in [24] and the model presented in [25]. Between 30 K and 60 K, the expansion responses just before and just after the first repetition are quite similar. However, just after 80 K, the cycled profile shows an abrupt change in the CTE, becoming nearly zero. These discontinuities in the CTE may be caused by the opening or closing of microcracks due to expansion, as described in [25].

In the case of thermal expansion after the third cycle, an asymmetric behavior is observed between the fibers oriented at 45° and -45°, with an almost negligible expansion occurring before 60 K. Beyond this point, a bifurcation in the strain response appears, showing compression along the -45° direction and tension along the 45° direction. This may be caused by a discontinuity in strain due to microcracking, potentially creating two asymmetric sublaminates, thus resulting in a bending-extension coupling. It can be observed in the case after the second repetition that even at low temperatures, the CTE can become negative. In carbon fibers, the differences in CTE are particularly significant precisely because of the inherently low or even negative thermal expansions. In the various works by [25], it is shown that the variation in the CTE can even change sign beyond a certain crack density ρ in the volume. Therefore, the results obtained here may be consistent with those findings.

Table II shows the different thermal expansion coefficients of the specimen after each repetition, for the temperature intervals 30–50 K and 90–150 K.

CONCLUSIONS

The development of efficient and safe hydrogen tanks is essential for the implementation of zero-emission aircraft. Among the various technological alternatives, Type V tanks represent the most promising option in terms of weight reduction and elimination of thermal compatibility issues between the liner and the composite. However, their main drawback remains hydrogen permeability caused by matrix microcracking, which compromises the system's tightness.

Since failure in these tanks is not defined by structural rupture but by their ability to maintain leak-

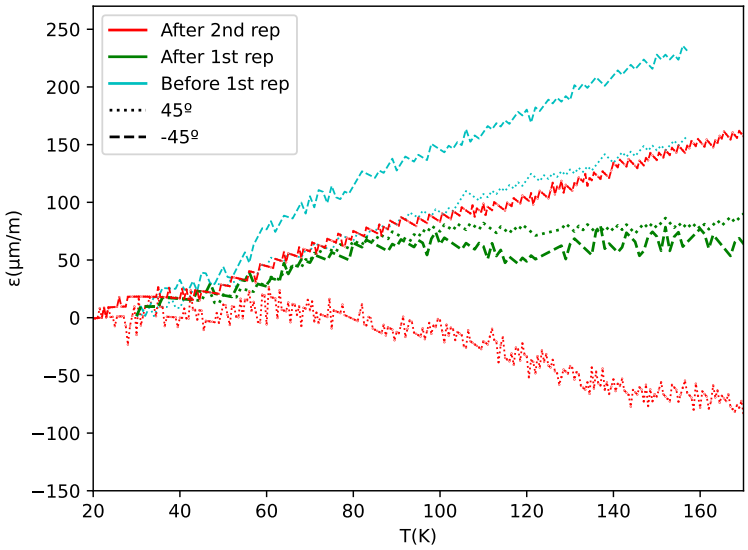

Figure 3. Thermal strain response in ± 45º directions

TABLE II. CTE values measured at different cycling states (α_0 before any cycles α_1 just after the first repetition and α_2 just after the second repetition.)

FBGS angle	$\alpha_0(10^{-6}m/mK)$	$\alpha_1(10^{-6}m/mK)$	$\alpha_2(10^{-6}m/mK)$	T_{inf} (K)	T_{sup} (K)
45º	1.38	0.51	0.027	20	50
	1.09	0.08	-1.15	90	140
-45º	1.64	0.85	0.65	20	50
	1.57	-0.06	0.91	90	140

tightness, it is crucial to develop structural health monitoring (SHM) systems capable of detecting the internal state of the material. Although technologies such as fiber Bragg grating sensors (FBGS) offer advantages such as low weight and electromagnetic immunity, their use for direct microcrack detection is still limited. Therefore, this work proposes an approach based on measuring the thermal expansion of the laminate as an indirect indicator of internal microcracking.

Experimental results show that the thermal expansion of the laminate changes significantly after microcrack damage that is induced at low temperatures. This phenomenon is consistent with previous micromechanical models and allows inference of the internal state of the material without destructive testing. Thus, thermal expansion measurements may serve as an effective tool for assessing the structural health of Type V tanks during operation, optimizing maintenance intervals, and enhancing safety in cryogenic hydrogen applications.

ACKNOWLEDGMENT

The work described in the paper has been financially supported by the Clean Aviation project FASTER-H2 (Project: 101101978)

REFERENCES

1. Sharma, G. D., M. Verma, B. Taheri, R. Chopra, and J. S. Parihar. 2023. "Socio-economic aspects of hydrogen energy: An integrative review," *Technological Forecasting and Social Change*, 192:122574, ISSN 00401625, doi:10.1016/j.techfore.2023.122574.
2. Bagarello, S., D. Campagna, and I. Benedetti. 2024. "A survey on hydrogen tanks for sustainable aviation," *Green Energy and Intelligent Transportation*:100224, ISSN 27731537, doi:10.1016/j.geits.2024.100224.
3. Niedermeyer, M. 2003. "X-33 LH2 Tank Failure Investigation Findings," .
4. Lee, J. A. and S. Woods. 2016. "Hydrogen Embrittlement," .
5. Azeem, M., H. H. Ya, M. A. Alam, M. Kumar, P. Stabla, M. Smolnicki, L. Gemi, R. Khan, T. Ahmed, Q. Ma, M. R. Sadique, A. A. Mokhtar, and M. Mustapha. 2022. "Application of Filament Winding Technology in Composite Pressure Vessels and Challenges: A Review," *Journal of Energy Storage*, 49:103468, ISSN 2352152X, doi:10.1016/j.est.2021.103468.
6. Mital, S. K., J. Z. Gyekenyesi, S. M. Arnold, R. M. Sullivan, J. M. Manderscheid, and P. L. N. Murthy. 2006. "Review of Current State of the Art and Key Design Issues With Potential Solutions for Liquid Hydrogen Cryogenic Storage Tank Structures for Aircraft Applications," .
7. Sharaf, O. Z. and M. F. Orhan. 2014. "An overview of fuel cell technology: Fundamentals and applications," *Renewable and Sustainable Energy Reviews*, 32:810–853, ISSN 1364-0321, doi:10.1016/j.rser.2014.01.012.
8. Mallick, K., J. Cronin, S. Arzberger, M. Tupper, L. Grimes-Ledesma, J. Lewis, C. Paul, and J. Welsh. 2004. "Ultralight Linerless Composite Tanks for In-Space Applications," in *Space 2004 Conference and Exhibit*, American Institute of Aeronautics and Astronautics, San Diego, California, ISBN 9781624100840, doi:10.2514/6.2004-5801.
9. Grimsley, B. W., R. J. Cano, N. J. Johnston, A. C. Loos, and W. M. McMahon. 2001. "Hybrid Composites for LH2 Fuel Tank Structure," .
10. Stokes, E. 2004. "Hydrogen Permeability of Polymer Based Composites Under Bi-axial Strain and Cryogenic Temperatures," in *45th AIAA/ASME/ASCE/AHS/ASC Structures, Structural Dynamics & Materials Conference*, American Institute of Aeronautics and Astronautics, Palm Springs, California, ISBN 9781624100796, doi:10.2514/6.2004-1858.
11. Condé-Wolter, J., M. G. Ruf, A. Liebsch, T. Lebelt, I. Koch, K. Drechsler, and M. Gude. 2023. "Hydrogen permeability of thermoplastic composites and liner systems for future mobility applications," *Composites Part A: Applied Science and Manufacturing*, 167:107446, ISSN 1359-835X, doi:10.1016/j.compositesa.2023.107446.
12. Greulich, O. R. 2017. "NASA Requirements for Ground-Based Pressure Vessels and Pressurized Systems (PVS)," .
13. Graue, R., M. Krisson, M. Erdmann, and A. Reutlinger. 2000. "Integrated Health Monitoring Approach for Reusable Cryogenic Tank Structures," *Journal of Spacecraft and Rockets*, 37(5):580–585, ISSN 0022-4650, 1533-6794, doi:10.2514/2.3630.
14. Gao, D., Z. Wu, L. Yang, Y. Zheng, and W. Yin. 2019. "Structural health monitoring for long-term aircraft storage tanks under cryogenic temperature," *Aerospace Science and Technology*, 92:881–891, ISSN 12709638, doi:10.1016/j.ast.2019.02.045.

15. Engberg, R. C. and T. K. Ooi. 2004. “Methods and piezoelectric imbedded sensors for damage detection in composite plates under ambient and cryogenic conditions,” San Diego, CA, p. 80, doi:10.1117/12.539276.
16. Liang, Z., D. Liu, X. Wang, J. Zhang, H. Wu, X. Qing, and Y. Wang. 2022. “FBG-based strain monitoring and temperature compensation for composite tank,” *Aerospace Science and Technology*, 127:107724, ISSN 12709638, doi:10.1016/j.ast.2022.107724.
17. Mizutani, T., N. Takeda, and H. Takeya. 2006. “On-board Strain Measurement of a Cryogenic Composite Tank Mounted on a Reusable Rocket using FBG Sensors,” *Structural Health Monitoring*, 5(3):205–214, ISSN 1475-9217, 1741-3168, doi:10.1177/1475921706058016.
18. Su, Y.-f., T.-y. Zhang, H. Sun, L.-h. Ma, and W. Zhou. 2024. “Cryogenic damage behavior of carbon fiber reinforced polymer composite laminates via fiber-optic acoustic emission,” *Composites Part A: Applied Science and Manufacturing*, 186:108435, ISSN 1359835X, doi:10.1016/j.compositesa.2024.108435.
19. Staszewski, W. J., C. Boller, and G. R. Tomlinson, eds. 2003. *Health Monitoring of Aerospace Structures: Smart Sensor Technologies and Signal Processing*, Wiley, 1 edn., ISBN 978-0-470-84340-6 978-0-470-09286-6, doi:10.1002/0470092866.
20. Flaggs, D. L. and M. H. Kural. 1982. “Experimental Determination of the In Situ Transverse Lamina Strength in Graphite/Epoxy Laminates,” *Journal of Composite Materials*, 16(2):103–116, ISSN 0021-9983, 1530-793X, doi:10.1177/002199838201600203.
21. Nairn, J. A. 2000. “Matrix Microcracking in Composites,” in *Comprehensive Composite Materials*, Elsevier, ISBN 9780080429939, pp. 403–432, doi:10.1016/B0-08-042993-9/00069-3.
22. Nairn, J. A., S. Hu, and J. S. Bark. 1993. “A critical evaluation of theories for predicting microcracking in composite laminates,” *Journal of Materials Science*, 28(18):5099–5111, ISSN 0022-2461, 1573-4803, doi:10.1007/BF00361186.
23. Nairn, J. A. 1989. “The Strain Energy Release Rate of Composite Microcracking: A Variational Approach,” *Journal of Composite Materials*, 23(11):1106–1129, ISSN 0021-9983, 1530-793X, doi:10.1177/002199838902301102.
24. Bowles, D. E. 1982. “The effects of microcracking on the thermal expansion of graphite-epoxy composites,” *Large Space Systems Technol., 1981*.
25. Hashin, Z. 1988. “Thermal expansion coefficients of cracked laminates,” *Composites Science and Technology*, 31(4):247–260, ISSN 02663538, doi:10.1016/0266-3538(88)90032-2.
26. Hashin, Z. 1986. “Analysis of stiffness reduction of cracked cross-ply laminates,” *Engineering Fracture Mechanics*, 25(5-6):771–778, ISSN 00137944, doi:10.1016/0013-7944(86)90040-8.
27. Talreja, R. 1985. “Transverse Cracking and Stiffness Reduction in Composite Laminates,” *Journal of Composite Materials*, 19(4):355–375, ISSN 0021-9983, 1530-793X, doi:10.1177/002199838501900404.
28. Nairn, J. A. 1992. “Microcracking, microcrack-induced delamination, and longitudinal splitting of advanced composite structures,” .
29. Hexcel. 2020. “HexPly M21 180°C (350°F) curing epoxy matrix,” Product Data Sheet, Hexcel.
30. Lakeshore, “DT-670 silicon diodes,” .
31. Gonzalez, M., J. M. Martinez Olmo, F. Terroba, F. Cabrerizo, A. Turon, J. Renart, and M. Frövel. 2024. “Thermal expansion calculation using FBGS in cryogenic applications,” *Cryogenics*, 142:103918, ISSN 0011-2275, doi:10.1016/j.cryogenics.2024.103918.
32. Corporation, E. T. 2024. “Model 3442 Miniature/Low Profile Extensometers,” Tech. Rep. 3442-010M-010M-LT.
33. Rosen, B. W. and Z. Hashin. 1970. “Effective thermal expansion coefficients and specific heats of composite materials,” *International Journal of Engineering Science*, 8(2):157–173, ISSN 0020-7225, doi:10.1016/0020-7225(70)90066-2.
34. Hashin, Z. 1985. “Analysis of cracked laminates: a variational approach,” *Mechanics of Materials*, 4(2):121–136, ISSN 01676636, doi:10.1016/0167-6636(85)90011-0.
35. Vinogradov, V. and Z. Hashin. 2010. “Variational analysis of cracked angle-ply laminates,” *Composites Science and Technology*, 70(4):638–646, ISSN 02663538, doi:10.1016/j.compscitech.2009.12.018.